



# HHS Public Access

Author manuscript

*J Neurointerv Surg.* Author manuscript; available in PMC 2016 April 01.

Published in final edited form as:

*J Neurointerv Surg.* 2015 April ; 7(4): 291–296. doi:10.1136/neurintsurg-2013-011076.

## Mechanical properties and fibrin characteristics of endovascular coil–clot complexes: relevance to endovascular cerebral aneurysm repair paradigms

Kevin J Haworth<sup>1,2</sup>, Christopher R Weidner<sup>2</sup>, Todd A Abruzzo<sup>1,3</sup>, Jason T Shearn<sup>2</sup>, and Christy K Holland<sup>1,2</sup>

<sup>1</sup>Division of Cardiovascular Health and Disease, Department of Internal Medicine, University of Cincinnati, Cincinnati, Ohio, USA

<sup>2</sup>Biomedical Engineering Program, University of Cincinnati, Cincinnati, Ohio, USA

<sup>3</sup>Department of Neurosurgery, University of Cincinnati, Cincinnati, Ohio, USA

### Abstract

**Background**—Although coil embolization is known to prevent rebleeding from acutely ruptured cerebral aneurysms, the underlying biological and mechanical mechanisms have not been characterized. We sought to determine if microcoil-dependent interactions with thrombus induce structural and mechanical changes in the adjacent fibrin network. Such changes could play an important role in the prevention of aneurysm rebleeding.

**Methods**—The stiffness of in vitro human blood clots and coil–clot complexes implanted into aneurysm phantoms were measured immediately after formation and after retraction for 3 days using unconfined uniaxial compression assays. Scanning electron microscopy of the coil–clot complexes showed the effect of coiling on clot structure.

**Results**—The coil packing densities achieved were in the range of clinical practice. Bare platinum coils increased clot stiffness relative to clot alone (Young's modulus 6.9 kPa and 0.83 kPa, respectively) but did not affect fibrin structure. Hydrogel-coated coils prevented formation of a clot and had no significant effect on clot stiffness (Young's modulus 2 kPa) relative to clot

---

To request permissions go to: <http://group.bmj.com/group/rights-licensing/permissions>

**Correspondence to.** Dr Kevin J Haworth, University of Cincinnati, Department of Internal Medicine, Cardiovascular Center Room 3939, 231 Albert Sabin Way, Cincinnati, OH 45267-0586, USA; kevin.haworth@uc.edu.

**Contributors** KJH co-designed and carried out analysis of all the data, drafted and revised the manuscript and is responsible for the overall content of the paper (in conjunction with CKH). CRW co-designed and carried out the experiments, assisted in data analysis and revised the manuscript. TAA co-designed and carried out the experiments including coil implantation, participated in data analysis and revised the manuscript. JTS co-designed and carried out the experiments and analysis related to compression testing and also revised the manuscript. CKH co-designed the experiments and analysis of all data, revised the manuscript and is responsible for the overall content of the paper (in conjunction with KJH).

**Competing interests** TAA has previously received consulting fees from Covidien-ev3 Endovascular and is currently a paid consultant for Microvention-Terumo.

**Provenance and peer review** Not commissioned; externally peer reviewed.

**Data sharing statement** All data from the study are included within this manuscript. Persons interested in these data should contact the corresponding author.

alone. Clot age decreased fiber density by 0.2 fibers/ $\mu\text{m}^2$  but not the stiffness of the bare platinum coil–clot complex.

**Conclusions**—The stiffness of coil–clot complexes is related to the summative stiffness of the fibrin network and associated microcoils. Hydrogel-coated coils exhibit significantly less stiffness due to the mechanical properties of the hydrogel and the inhibition of fibrin network formation by the hydrogel. These findings have important implications for the design and engineering of aneurysm occlusion devices.

---

## INTRODUCTION

In recent decades, endovascular therapies have evolved for the treatment of intracranial aneurysms. Endosaccular coil embolization forms the cornerstone of this treatment paradigm. The safety and efficacy of this procedure in the prevention of rebleeding from ruptured aneurysms has been proven in randomized clinical trials.<sup>1</sup> Coil embolization relies on the implantation of microcoils into the lumen of an aneurysm sac. The microcoils promote thrombus formation in the aneurysm, thereby preventing the entry of blood flow. Early aneurysm rupture after coil embolization is a rare event.<sup>2</sup> Newer endovascular aneurysm therapies based on parent vessel reconstruction with flow-diverting stents have been associated with early post-procedural aneurysm rupture despite observing aneurysm occlusion using angiography.<sup>3,4</sup> Unlike coil embolization, these therapies rely on endosaccular thrombus alone for aneurysm occlusion. Reports of postoperative aneurysm rupture after treatment with flow-diverting implants suggest that endosaccular thrombus alone is insufficient to protect against aneurysm rupture.

Microcoil implantation can significantly affect endosaccular thrombus properties. Killer *et al*<sup>5</sup> found that bare platinum coils stimulate more thrombus formation than HydroCoils, but HydroCoils produce a greater volumetric fill than bare platinum coils. The mechanical properties of coil–clot complexes can, in turn, affect aneurysm wall stress and potentially play an important role in the prevention of aneurysmal bleeding. Ramachandran<sup>6</sup> used a finite element model to show that aneurysm wall stress decreases as the Young's modulus of the filling material inside an aneurysm increases. Such models can be used to estimate aneurysm stress alterations that take place as a result of coil embolization. The stiffness of coil–clot complexes has not been measured and therefore the amount of aneurysm wall stress reduction that can be expected after coil embolization is unknown.

Our study was designed to elucidate the role of microcoils on the structure and stiffness of the coil–clot complex. Scanning electron microscopy (SEM) images were used to determine the thickness and density of individual fibers within fibrin networks. The stiffness of the coil–clot complex was quantified using Young's modulus, which was computed from the results of an unconfined uniaxial compression test. The hypothesis tested was that coil–clot complexes have a greater stiffness than clot alone and that the addition of coils does not alter the fibrin characteristics.

## MATERIALS AND METHODS

To determine the effects of platinum microcoils and hydrogel-coated microcoils on the structural organization of the intrinsic fibrin network and on the mechanical properties of human whole blood clots, microcoils were deposited into in vitro aneurysm phantoms comprised of glass 96-well plates. Blood was added to the wells and allowed to clot. Each coil-clot complex was removed from the phantom and tested mechanically by uniaxial compression and imaged with SEM.

All bare platinum coils used in these experiments were NXT detachable coils (Covidien-ev3 Endovascular, Plymouth, Minnesota, USA). In aneurysm phantoms treated with bare platinum coils, the initial framing coil placed was a standard Tetris 3-D TS coil (Covidien-ev3 Endovascular), and subsequent filling coils were Helix soft coils (Covidien-ev3 Endovascular). All hydrogel-coated coils used in these experiments were HydroCoil 14 detachable microcoils (Microvention-Terumo, Tustin, California, USA).

### Coil deployment

A deployment cap made from a glass rod restrained the coils in each well. Each cylindrical well was 3 mm deep and 7.7 mm in diameter, confining the coil-clot complexes to a volume of 0.14 mL. The size of the aneurysm space is similar to a human cerebral berry aneurysm.<sup>5</sup> The cylindrical space allowed modeling of the compression data to determine the Young's modulus.<sup>7</sup>

All microcoils were separated from their pusher wires prior to implantation in aneurysm phantoms. HydroCoils were separated using the HydroLink detachment system. Four coils were deployed into each cylindrical space. The framing coil had a deployed major diameter of 8 mm, with the other three coils of increasingly smaller major diameters. The deployed major diameters of the smaller filling coils were between 2 and 6 mm. For the smallest bare platinum coils, the major diameter was either 2 mm or 3 mm. The total length of the bare platinum coils and HydroCoils implanted was 36 and 38 cm, respectively. The bare platinum coils use Nitinol filament technology, which is designed to provide shape memory and prevent coil compaction. In order to model the process of coil embolization as it is performed clinically, each aneurysm phantom was packed as tightly as possible using a prespecified coil type. The packing density of each coil-clot complex was determined from the final dimensions and calculated volume of the coils based on the manufacturers' specifications. The HydroCoil volume was calculated based on the expanded volume of the hydrogel coating.

### Clot production

The clot production protocol was based on the work of Holland *et al.*<sup>8</sup> This model creates reproducible clots well suited to comparative studies.<sup>9-11</sup> Human whole blood was drawn from five healthy volunteers following a protocol approved by the Institutional Review Board. For each coil-clot combination described below, one blood clot was made from each of the five subjects, resulting in five samples per combination. After deploying the coils (for experimental groups with coils), 0.12 mL of blood was pipetted into each in vitro aneurysm

space. The expansion of the HydroCoil in the in vitro aneurysm space, once exposed to blood, displaced about 15% of the injected blood volume. The deployment cap was replaced with a solid glass cap. The glass plate was covered with Parafilm (Bemis Company, Neenah, Wisconsin, USA) and placed in a 37°C water bath for 3 h to stimulate the clotting cascade. After the 3 h incubation, coil–clot complexes were either mechanically tested or stored at 5°C in a refrigerator for 3 days to allow for additional retraction. Three-day-old coil–clot complexes were also mechanically tested. Coil–clot complexes were stored at 5°C to reduce bacterial growth and inhibit enzymatic activity that could change fibrin network in a variable manner. Furthermore, cellular metabolism is decreased at 5°C, reducing the formation of echinocytes. However, storage at 5°C does result in platelet activation in a manner similar to that observed in patients with cardiovascular disease.<sup>12</sup> Although, as noted above, the major diameter of the smaller coils changed between samples, the changes were the same between each age group so that the average stiffness and fiber characteristics could be compared between age groups.

### Mechanical testing

The coil–clot complexes were removed from the 96-well plate and immediately placed in 0.01 M phosphate-buffered saline (PBS) at 22±2°C. The coil–clot complex diameter and height were measured with digital calipers. Stiffness measurements were made with a TestResources 100R system (TestResources, Shakopee, Minnesota, USA) with a 10 N load cell. The coil–clot complexes were tested in unconfined uniaxial compression. They were compressed 10 times, oscillating between a 1% and 3% strain over a 10 s period, to reduce the effects of hysteresis. Three strain levels were tested: 10%, 20% and 30%. The coil–clot complexes were allowed to recover for 10 min before the next strain level was applied.

### Clot stiffness model

The Mooney–Rivlin and Neo-Hookean hyperelastic models were used to model the coil–clot complexes. The Mooney–Rivlin and Neo-Hookean models have been used to describe rubbers and rubber-like materials.<sup>13,14</sup> Biologic soft tissues are nearly incompressible and exhibit elastic deformations similar to rubbers. Corbett *et al*<sup>15</sup> created an aneurysm thrombus analog from silicone rubber with similar properties to excised thrombus. Karšaj and Humphrey used a Neo-Hookean model for early stage thrombus.<sup>16</sup>

The engineering stress ( $S$ ) for a cylindrical sample undergoing unconstrained uniaxial compression along its height is described using the Mooney–Rivlin model as follows:<sup>17</sup>

$$S = \mu_1(\lambda - \lambda^{-2}) + \mu_2(\lambda - \lambda^{-3}). \quad (1)$$

where  $\lambda$  is the stretch ratio and  $\mu_1$  and  $\mu_2$  are the Mooney–Rivlin constants. This model was fit to the experimental data and the constants determined. The Neo-Hookean model is a derivative of the Mooney–Rivlin model where the second material parameter ( $\mu_2$ ) is set to zero before applying a fit to determine  $\mu_1$ .<sup>18</sup> Data were fit individually to each sample. Using the derived constants and an assumed Poisson's ratio ( $\nu$ ) for an incompressible material of 0.4995, the Young's modulus ( $E$ ) was determined as:<sup>17</sup>

$$E=2(\mu_1+\mu_2)(1+\nu). \quad (2)$$

### Clot preparation for SEM

After mechanical testing, each coil–clot complex was prepared for SEM using a protocol similar to that described by Bray.<sup>19</sup> The coil–clot complex was submerged in 1 mL of 2% glutaraldehyde in 0.1 M cacodylate buffer and placed in a 5°C refrigerator overnight. The coil–clot complex was washed in cacodylate buffer twice for 10 min each and fixed in 1% osmium tetroxide in 0.1 M cacodylate buffer for 2±1 h. The coil–clot complex was washed with deionized water twice for 15 min each. Next, the coil–clot complexes were run through alcohol dehydration stages for 1 h at each of the following ethanol concentrations: 50%, 75%, 95% and 100%. A final dehydration for 12 h was performed in 100% ethanol. Finally, the coil–clot complex was chemically dried by washing in propylene oxide for 2±1 h. The dehydrated coil–clot complexes were allowed to air-dry in a fume hood on filter paper overnight. Coil–clot complexes were sputter-coated with gold to improve SEM image contrast.

### SEM of coil–clot complexes

SEM (Philips XL 30-ESEM, FEI Company, Hillsboro, Oregon, USA) was performed in high vacuum mode. Five images were taken of each coil–clot complex at locations in the center and at 12, 3, 6 and 9 o'clock positions. The 3 and 6 o'clock position images were centrally located and the 12 and 9 o'clock images were near the edge of the coil–clot complex. The location of the SEM images was standardized to reduce user bias and to include the range of fibrin characteristics due to coil–clot complex inhomogeneity. Control SEM images of a HydroCoil without a clot were taken to determine the effect of the fixation process on the HydroCoil. SEM images of the HydroCoil were acquired at a location where the hydrogel was intact.

### Image processing

The diameter and density of fibrin fibers was derived from the SEM images. A 3 µm × 3 µm grid was superimposed on the image in order to define regions of interest (ROIs). Measurements were taken within randomly selected ROIs by observers blinded to the type and age of each coil–clot complex. The diameter of each fibrin strand and the total number of fibrin strands within the ROI were measured and the average of each measurement was calculated.

### Statistical analysis

The statistical package R (R Development Core Team, R Foundation for Statistical Computing, Vienna, Austria) was used for all statistical analyses. Data were analyzed for significance using the mixed-effects model (Package: *nlme* and function: *lme*) that accounted for correlations between the groups by matching the data to the subjects in addition to treatment group. Post hoc power of the statistical test between coil–clot complex types was computed from the paired and two-sided t test in R. Statistical significance was defined as  $p < 0.05$ . The fits reached convergence for all datasets for both the Mooney–

Rivlin and Neo-Hookean models. For each sample, the fitted values for  $\mu_1$  and  $\mu_2$  did not depend on the initial guesses for the fit. In all cases, the Mooney–Rivlin model fit the data with an  $R^2$  value 0.98 and the Neo-Hookean model fit the data with an  $R^2$  value 0.79. All subsequent results are reported for the Mooney–Rivlin model because of the superior  $R^2$  fit to the data.

## RESULTS

### Coil packing density

The percentage of the aneurysm space filled for the bare platinum coils and the HydroCoils was  $14.6 \pm 1.6\%$  and  $58.5 \pm 10.5\%$ , respectively. These volume fill fractions are within the range achieved in clinical practice.<sup>20</sup>

### Stiffness testing

Each strain level resulted in qualitatively similar results. The bare platinum coil–clot complexes were markedly stiffer than either the HydroCoil–clot complex or the clot alone (figure 1).

A post hoc power analysis indicated that all statistical results had  $>90\%$  power unless otherwise noted. The results of the mixed-effects model showed that the maximum stress of the bare platinum coil–clot complexes was statistically different from both clots alone and HydroCoil–clot complexes. The material constants  $\mu_1$  and  $\mu_2$  obtained from fitting the individual 30% strain data, the computed Young's modulus and maximum stress are reported in table 1. Box plots of the Young's modulus data are shown in figure 1. The mean  $\pm$ SD Young's modulus values for the 3 h time points were  $0.83 \pm 0.71$  kPa,  $6.9 \pm 7.4$  kPa and  $2.0 \pm 1.8$  kPa for the clot alone, bare platinum coil–clot complex and HydroCoil–clot complex, respectively. For the 3-day-old clots, the Young's modulus values were  $0.44 \pm 0.45$  kPa,  $2.3 \pm 2.2$  kPa and  $2.0 \pm 1.9$  kPa for the clot alone, bare platinum coil–clot complex and HydroCoil–clot complex, respectively. The mixed-effects model showed that there was no significant difference between the two clot ages ( $p > 0.05$ ) for the Young's modulus. The comparison between clots alone and HydroCoil–clot complexes did not reveal a statistically significant difference. However, the Young's modulus for the bare platinum coil–clot complex was significantly different from both the HydroCoil–clot complexes and the clots alone ( $p < 0.05$ ).

### SEM images

Figure 2 shows representative SEM images of the bare platinum coil and HydroCoil after exposure to whole blood and fixation. The hydrogel can be seen in figure 2A and C as the smooth coating on the coil. After clotting and retracting for 3 days, erythrocytes without fibrin were observed for the HydroCoil–clot complexes (figure 2A,C). In comparison, the bare platinum coil showed a mature fibrin mesh after retracting for 3 days (figure 2B,D).

Figure 3 shows representative SEM images of a clot alone (figure 3B,D) and the bare platinum–coil complex (figure 3A,C). These representative images demonstrate the qualitative similarity of the clot produced with and without the bare platinum coil. Table 2

shows the number of fibrin strands/ $\mu\text{m}^2$  and the average fibrin diameter observed in the clot alone and the bare platinum coil–clot complexes. The HydroCoil–clot complexes are not included in the table because no fibrin was observed. Using the mixed-effects model, no significant difference in fibrin diameter or fibrin density was found between the coil–clot complexes ( $p > 0.05$ ). A statistically significant difference in fibrin density and fibrin diameters was found between the two clot ages. The statistical power for the fibrin density and fibrin diameters was 70% and 46%, respectively, with an  $\alpha$  of 0.05.

## DISCUSSION

The hypothesis tested in this study was that coil–clot complexes have a greater stiffness than clot alone and that the addition of coils does not alter the fibrin characteristics. Testing this hypothesis was, in part, motivated by simulations indicating that aneurysm wall stress is reduced as the stiffness of the aneurysm filling material increases.<sup>6</sup> The presence of bare platinum coils in clots increased the complex stiffness but did not change the fibrin diameter or fibrin density relative to clots alone. The increase in stiffness observed with the mechanical measurements is probably due to a summative effect of the fibrin network and the coil because the fibrin structure did not change as a result of coil implantation. It should be noted that the images were of the coil–clot complex surface, so it is possible that the fibrin structure within the coil–clot complex is different. The fibrin fiber density and diameter was different for coil–clot complexes that were 3 h old and those that were 3 days old for both the bare platinum coil–clot complexes and the clots alone, indicating that clot formation and retraction was a dynamic process. However, the changes are relatively small, even though they are statistically significant, and this may be the reason that no change in the stiffness over time was observed. The implantation of HydroCoils prevented the establishment of a fibrin network altogether. Scant erythrocyte adhesion to the HydroCoils, however, was evident. The HydroCoil–clot complex and the clot alone yielded very similar stiffnesses even though the source of the stiffness—the fibrin network for the clot alone and the metal coils for the HydroCoil—were different.

The lack of fibrin formation associated with HydroCoils was also observed histologically by Killer *et al*<sup>5</sup> in an in vivo aneurysm model. Our SEM data confirm that the hydrogel reduces fibrin formation. Killer *et al* also noted that the hydrogel helped fill a larger volume fraction of the aneurysm. The packing density for bare platinum coils ( $14.6 \pm 1.6\%$ ) was significantly lower than for the HydroCoil ( $58.5 \pm 10.5\%$ ). This difference in packing density could also have affected the contribution of the coil to the stiffness of the coil–clot complex. An even stiffer coil–clot complex might have been produced if the packing density of the bare platinum coils had been higher. However, increasing the bare platinum coil packing density to an equivalent HydroCoil packing density would result in a deployment strategy that would put the aneurysm at risk of rupture.<sup>20</sup> The stiffness of a bare platinum coil–clot complex with a high (nonclinical) packing density would probably be insufficient to impart a reduction in aneurysmal wall sac strength.<sup>6</sup>

The impact of filling material stiffness on aneurysm wall stress was shown by Ramachandran.<sup>6</sup> Based on his simulations, wall stress is reduced even when the aneurysm is only partially occluded. The magnitude of wall stress reduction is strongly dependent on the

stiffness of the filling material. The Young's modulus values determined in this study are similar to the lowest stiffness values considered by Ramachandran.<sup>6</sup> These stiffness values were not predicted to reduce aneurysm wall tension. Such a low stiffness value implies that the effect of wall tension is probably not an important factor in the mural stabilization of acutely ruptured aneurysms after coil embolization.

There are several factors that may limit the generalization of these in vitro results to the in vivo environment. The sub-failure mechanical properties of each coil-clot complex were measured first, and the complexes were dehydrated for SEM analysis thereafter. The compression measurements may have resulted in compaction of the fibrin strands, resulting in an artificially high fibrin density across all coil-clot combinations. Additionally, in this study, PBS was used to hydrate the coil-clot complex whereas in vivo a thrombus would be surrounded by whole blood. The use of PBS for hydration also eliminated the presence of endogenous thrombogenic and thrombolytic molecules that are present in plasma and whole blood. The presence of these endogenous molecules might lead to a change in thrombus properties over time, which was not included in the in vitro study. Similarly, stiffness tests were performed at 22°C instead of 37°C, which would retard thrombogenic or thrombolytic activity.<sup>21</sup>

The reported Young's modulus values were derived based on the Mooney-Rivlin hyperelastic model. This model assumes a perfect cylindrical shape and an isotropic material. These assumptions may have been imperfect, particularly for the clots with HydroCoils or bare platinum coils that are designed to take on a spheroid shape when deployed. The model also required the dimensions of the coil-clot complex, which were measured using digital calipers. The uncertainty in these measurements probably contributed to the variance in the measurements. However, the trend among coil-clot complexes for the Young's modulus and maximum stress at 30% strain are the same, which implies that the qualitative conclusions drawn are still valid.

## CONCLUSIONS

This study is an initial development in understanding the complex clotting response to aneurysm coils. The HydroCoil-clot complexes and the clots without coils had similar stiffnesses, but the bare platinum coil-clot complexes were much stiffer. The presence of bare platinum coil did not affect the fibrin mesh characteristics of the coil-clot complex. The effect of hemodynamic parameters or blood chemistry on the coil-clot complex integrity was not investigated in this study, but could be a point of emphasis in future work.

## Acknowledgements

The authors acknowledge Covidien-ev3 Endovascular for donation of the bare platinum coils and Microvention-Terumo for donation of the HydroCoils. Christina L Bennett-Stamper of the USA Environmental Protection Agency is acknowledged for her assistance with tissue preparation for SEM and Marepalli Rao of the University of Cincinnati is acknowledged for fruitful discussions regarding statistical analysis.

**Funding** This work was supported by the National Institutes of Health grants numbers R01 NS047603 and F32 HL104916 and the University of Cincinnati.



## REFERENCES

1. Molyneux A. International Subarachnoid Aneurysm Trial (ISAT) of neurosurgical clipping versus endovascular coiling in 2143 patients with ruptured intracranial aneurysms: a randomised trial. *Lancet*. 2002; 360:1267–1274. [PubMed: 12414200]
2. White PM, Lewis SC, Nahser H, et al. HydroCoil Endovascular Aneurysm Occlusion and Packing Study (HELPS trial): procedural safety and operator-assessed efficacy results. *AJNR Am J Neuroradiol*. 2008; 29:217–223. [PubMed: 18184832]
3. Saatci I, Yavuz K, Ozer C, et al. Treatment of intracranial aneurysms using the pipeline flow-diverter embolization device: a single-center experience with long-term follow-up results. *AJNR Am J Neuroradiol*. 2012; 33:1436–1446. [PubMed: 22821921]
4. Cebal JR, Mut F, Raschi M, et al. Aneurysm rupture following treatment with flow-diverting stents: computational hemodynamics analysis of treatment. *AJNR Am J Neuroradiol*. 2011; 32:27–33. [PubMed: 21071533]
5. Killer M, Plenk H, Minnick B, et al. Histological demonstration of healing in experimental aneurysms. *Minim Invasive Neurosurg*. 2009; 52:170–175. [PubMed: 19838970]
6. Ramachandran R. A nonlinear stress sensitivity study on role of coil-thrombus complex in reduction of idealized cerebral aneurysm wall stresses. 2008 [http://rave.ohiolink.edu/etdc/view?acc\\_num=ucin1202193853](http://rave.ohiolink.edu/etdc/view?acc_num=ucin1202193853).
7. Cohen B, Lai WM, Mow VC. A transversely isotropic biphasic model for unconfined compression of growth plate and chondroepiphysis. *J Biomech Eng*. 1998; 120:491–496. [PubMed: 10412420]
8. Holland CK, Vaidya SS, Datta S, et al. Ultrasound-enhanced tissue plasminogen activator thrombolysis in an in vitro porcine clot model. *Thromb Res*. 2008; 121:663–673. [PubMed: 17854867]
9. Datta S, Coussios C-C, Ammi AY, et al. Ultrasound-enhanced thrombolysis using definitivity as a cavitation nucleation agent. *Ultrasound Med Biol*. 2008; 34:1421–1433. [PubMed: 18378380]
10. Hitchcock KE, Ivancevich NM, Haworth KJ, et al. Ultrasound-enhanced rt-PA thrombolysis in an ex vivo porcine carotid artery model. *Ultrasound Med Biol*. 2011; 37:1240–1251. [PubMed: 21723448]
11. Sutton JT, Ivancevich NM, Perrin SR, et al. Clot retraction affects the extent of ultrasound-enhanced thrombolysis in an ex vivo porcine thrombosis model. *Ultrasound Med Biol*. 2013; 39:813–824. [PubMed: 23453629]
12. Ayukawa O, Nakamura K, Kariyazono H, et al. Enhanced platelet responsiveness due to chilling and its relation to CD40 ligand level and platelet-leukocyte aggregate formation. *Blood Coagul Fibrinolysis*. 2009; 20:176–184. [PubMed: 19300046]
13. Mooney M. A theory of large elastic deformation. *J Appl Phys*. 1940; 11:582–592.
14. Rivlin RS. Large elastic deformations of isotropic materials. I. Fundamental concepts. *Philos Trans R Soc A*. 1948; 240:459–490.
15. Corbett TJ, Doyle BJ, Callanan A, et al. Engineering silicone rubbers for in vitro studies: creating AAA models and ILT analogues with physiological properties. *J Biomech Eng*. 2010; 132:011008. [PubMed: 20524746]
16. Karšaj I, Humphrey JD. A mathematical model of evolving mechanical properties of intraluminal thrombus. *Biorheology*. 2009; 46:509–527. [PubMed: 20164633]
17. Bower, AF. *Applied Mechanics of Solids*. CRC Press; 2011.
18. Treloar LRG. Stresses and birefringence in rubber subjected to general homogeneous strain. *Proc Phys Soc*. 1948; 60:135–144.
19. Bray D. Critical point drying of biological specimens for scanning electron microscopy. *Supercritical Fluid Methods Protoc*. 2000; 13:235–243.
20. Tamatani S, Ito T, Abe H, et al. Evaluation of the stability of aneurysms after embolization using detachable coils: correlation between stability of aneurysms and embolized volume of aneurysms. *AJNR Am J Neuroradiol*. 2002; 23:762–767. [PubMed: 12006273]
21. Brecher G, Bessis M. Present status of spiculed red cells and their relationship to the discocyte-echinocyte transformation: a critical review. *Blood*. 1972; 40:333–344. [PubMed: 5056966]

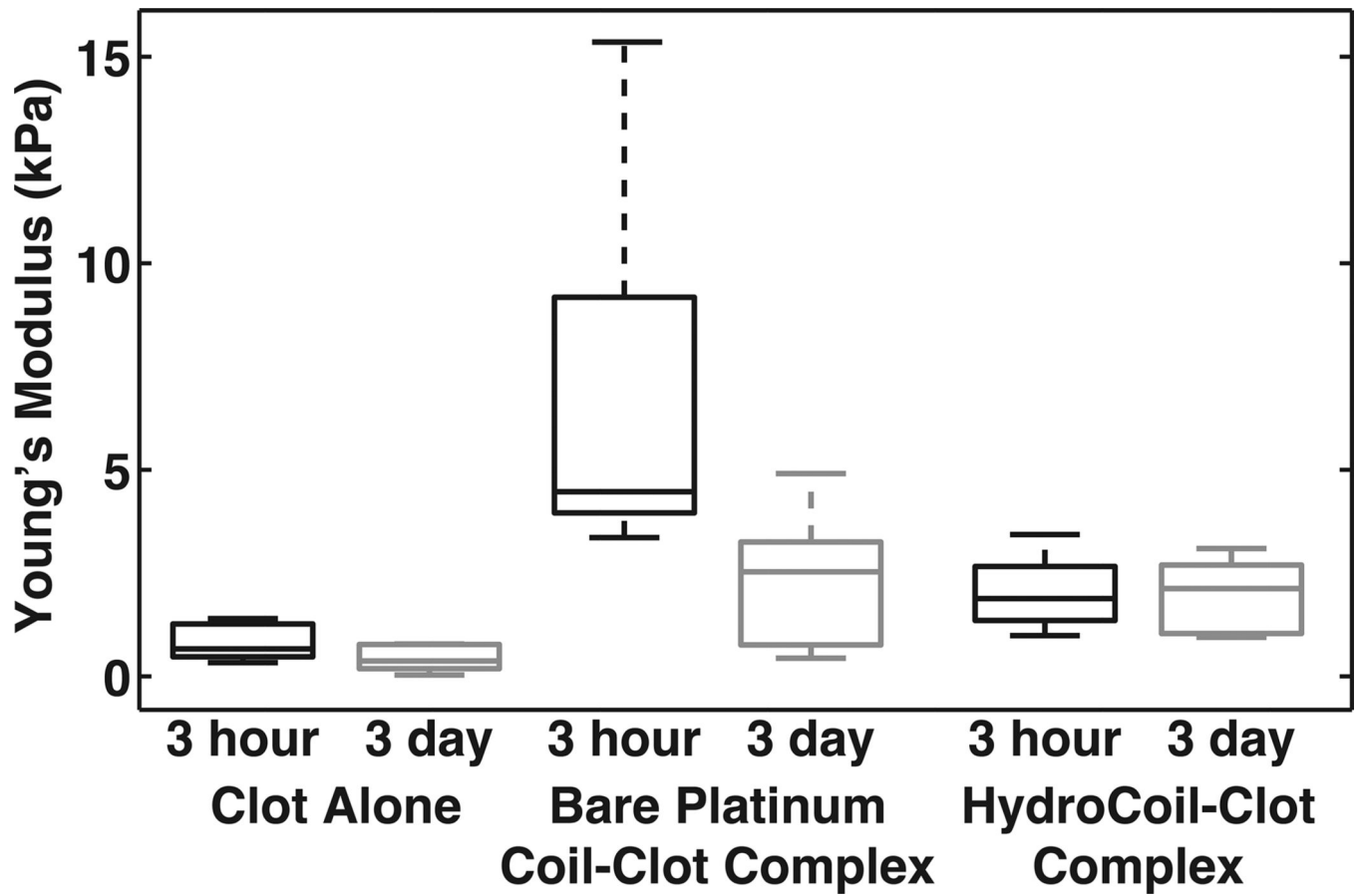


**Figure 1.** Average Young's modulus from the 30% strain data determined from the Mooney–Rivlin constants and Equation. The whiskers indicate the extreme measurements, the box indicates the 25<sup>th</sup> and 75<sup>th</sup> percentiles and the line within the box is the median value.

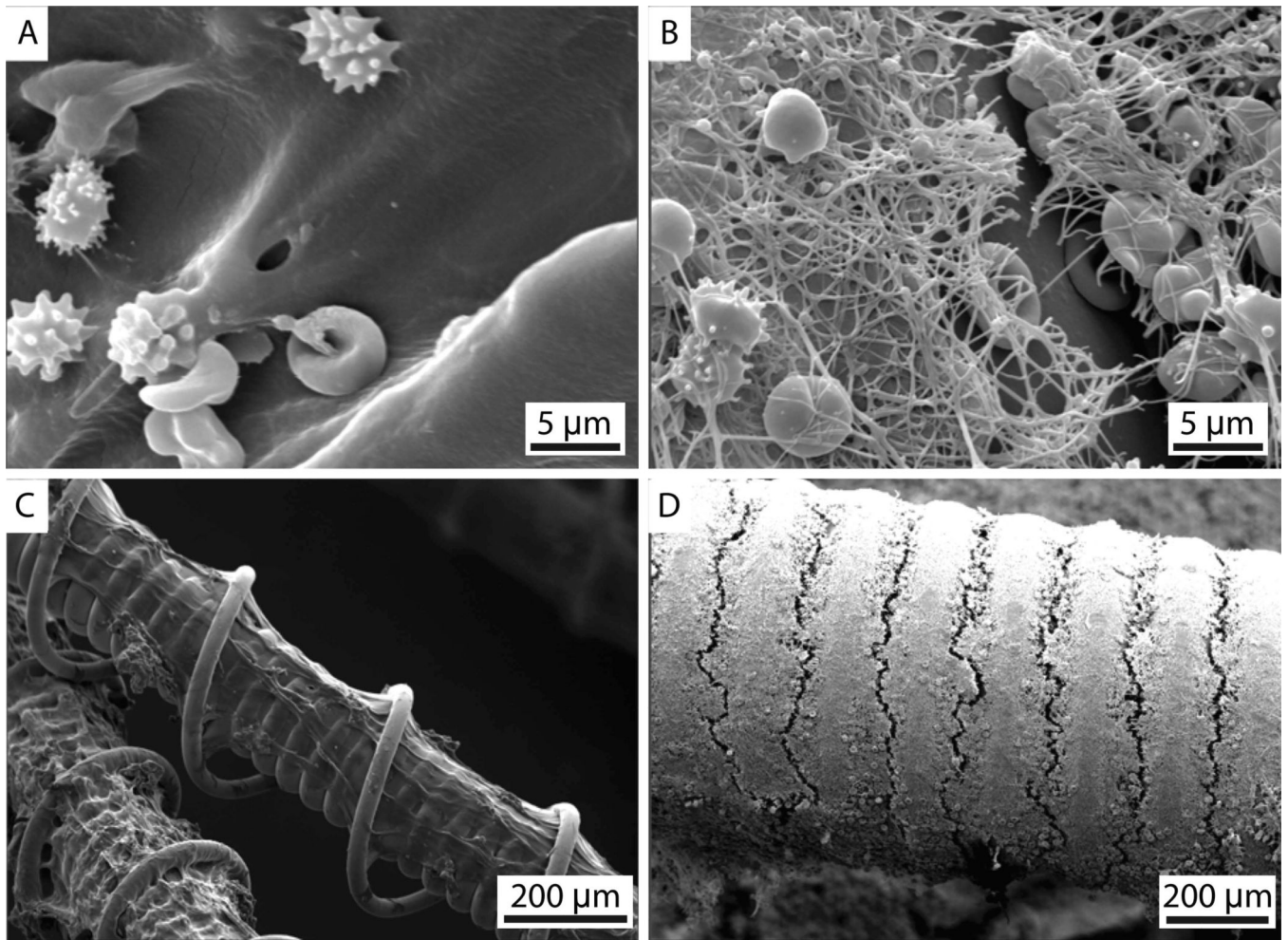


**Figure 2.** Scanning electron microscopy images of a HydroCoil-coil-clot complex and a bare platinum coil-clot complex. (A) HydroCoil-coil-clot complex and (B) bare platinum coil-clot complex at 3500× magnification, (C) HydroCoil-coil-clot complex at 120× magnification and (D) bare platinum coil-clot complex at 100× magnification.

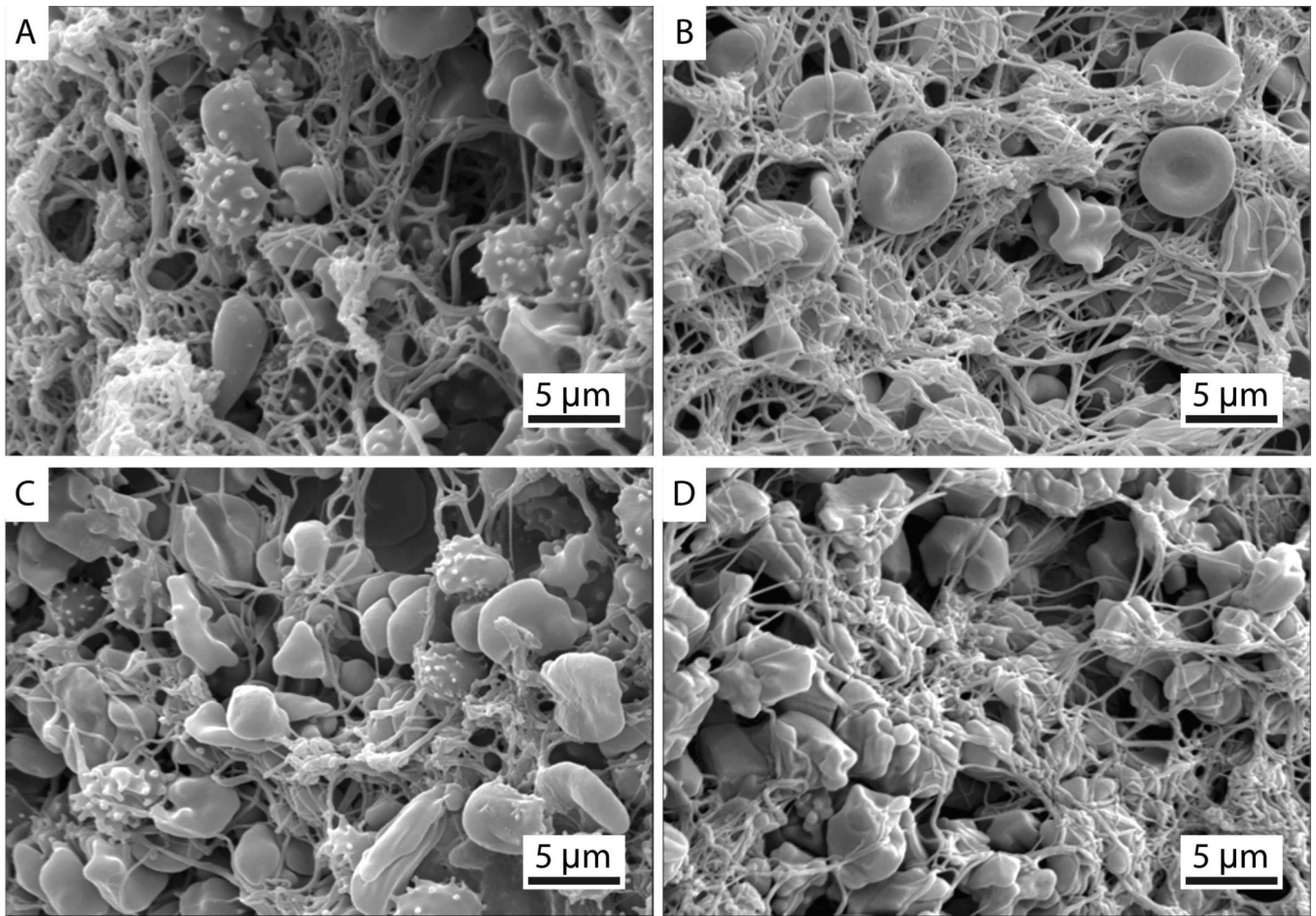


**Figure 3.** Representative scanning electron microscopy images of (A, C) bare platinum coil-clot complexes and (B, D) clots alone. All images are at 3500× magnification. Echinocytes (speculated red blood cells) are present due to the diminishing supply of ATP during blood clot formation and storage at 5°C.

**Table 1**

Average maximum stress and Mooney–Rivlin constants at 30% strain for each coil–clot complex type

	<b>Clot alone</b>	<b>Bare platinum coil–clot complex</b>	<b>HydroCoil–clot complex</b>
Maximum stress (Pa)			
3 h	310±120	4240±1260	900±560
3 days	330±150	2680±1660	940±400
$\mu_1$ (Pa)			
3 h	360±340	-460±4020	540±890
3 days	-110±610	-2740±2190	380±820
$\mu_2$ (Pa)			
3 h	-80±190	2760±2600	140±810
3 days	260±500	3500±2360	270±650

Author Manuscript

Author Manuscript

Author Manuscript

Author Manuscript

**Table 2**

Average fibrin density and average fibrin fiber diameter of clot alone and bare platinum coil–clot complexes

	Density (fibers/ $\mu\text{m}^2$ )	Fiber diameter ( $\mu\text{m}$ )
Clot alone		
3 h	0.86 $\pm$ 0.22	0.24 $\pm$ 0.03
3 days	0.65 $\pm$ 0.35	0.21 $\pm$ 0.03
Bare platinum coil–clot complex		
3 h	0.99 $\pm$ 0.21	0.21 $\pm$ 0.01
3 days	0.78 $\pm$ 0.26	0.20 $\pm$ 0.02

Author Manuscript

Author Manuscript

Author Manuscript

Author Manuscript